Removal of microcystin-LR and other water pollutants using sand coated with bio-optimized carbon submicron particles: Graphene oxide and reduced graphene oxide

Pratik Kumar [a], José Alberto Espejel Pérez [b], Maximiliano Cledon [c], Satinder Kaur Brar [a,d,*], Sung Vo Duy [e], Sébastien Sauvé [e], Émile Knystautas [f]

[a] INRS-ETE, Université du Québec, 490, Rue de la Couronne, Québec G1K 9A9, Canada
[b] Facultad de Ciencias Quimicas, Universidad La Salle Mexico, Benjamin Franklin 45, Cuauhtemoc, Mexico City 06140, Mexico
[c] CIMAS (CONICET, UnComa, Rio Negro), Güemes 1030, San Antonio Oeste, Rio Negro, Argentina
[d] Department of Civil Engineering, Lassonde School of Engineering, York University, North York, Toronto M3J 1P3, Ontario, Canada
[e] Department of Chemistry, Université de Montréal, Montreal H3C 3J7, Canada
[f] Department of Physics, Engineering Physics and Optics, Université Laval, 1045 Avenue de la Médecine, Québec G1V 0A6, Canada

ARTICLE INFO

ABSTRACT

Sand is the most used filter adsorbent material in a drinking water treatment plant (DWTP) or household purpose filters. However, sand poses challenge for the micropollutant removal in presence of metals, natural organic matter, total organic carbon, ammonia and other macro-pollutants. In this study, sand was coated using laboratory-synthesized graphene oxide (GO) and reduced graphene oxide (rGO) to enhance its surface properties in terms of hydrophobicity, roughness and specific surface area (6 times higher for GO/rGO as compared to 5.5 m^2/g for sand), that allowed an enhanced adsorption of macro pollutants as well as one target micropollutant: Microcystin-LR (MC-LR). A more electropositive surface than sand (zeta potential: −43.2 mV) in form of iron oxide-coated sand (IOCS or Fe: −21.2 mV) and its combination with GO (FeGO: −13.4 mV) was tested to validate the hypothesis of enhanced MC-LR adsorption due to electrostatic attraction. Two known MC-LR degraders (*Arthrobacter ramosus* and *Bacillus* sp.) were screened before bioaugmentation, based on the biofilm forming potential for each coated sand composite. Additionally, the dosage of GO and rGO were bio-optimized before coating them over the sand grains (400 mg/L for GO and 520 mg/L for rGO), to obtain a non-toxic and non-disruptive effect and providing at least 60% cell viability. A highest MC-LR removal of 91% was obtained under biodegradation phase using rGO-coated sand that showed an increase of 47.2% in MC-LR removal when compared to physical adsorption phase. Sand filter (control) showed a maximum MC-LR removal of 54.7%. The highest saturation adsorbent constants of 8.5 mg/kg and 7.4 mg/kg were obtained for GO and rGO-coated sand media, respectively, which was 5–6 times higher than the uncoated sand.

1. Introduction

The filtration unit forms a major treatment module in the drinking water treatment plant (DWTPs) chain. The majority of the DWTPs consists of sand as the primary filter media which adsorbs metals ions, sediments and organic matter, thus providing an economical and quick treatment solution [1]. However, sand as a filter media presents certain limitations, mainly because of its low adsorption capacity and may only provide partial removal of water pollutants, especially the emerging contaminants. The stringent water quality guidelines for some highly toxic emerging contaminants such as the hepatotoxic Microcystin-LR at <1 μg/L (WHO), makes sand media questionable in the context of the modern drinking water treatment aspects. A low surface area and pla-

nar morphology of sand is often responsible for the low water pollutant removal [2–3].

In this study, use of graphene oxide (GO) and reduced graphene oxide (rGO) submicron particles is explored to enhance the adsorption performance of quartz sand by thermal coating. Various studies have shown the potential of these sub-micron materials for the removal of diverse water contaminants [4–6]. Commercialized carbon source adsorbents such as granulated activated carbon have shown less contaminant removal (~60%) for pharmaceutical mixtures as compared to GO (96%) [7]. However, use of only GO as an adsorbent could be uneconomical and time-consuming, delivering a high empty bed contact time during the filter operation in a DWTPs. Hence, coating them over bigger size particles such as sand, could be a suitable alternative. Graphene oxide coated over sand was shown to effectively re-

move metal ions, natural organic matter: NOMs and organic carbon [8,9]. However, the removal of cyanotoxins has not been explored to date. How these modified sand surfaces behave for cyanotoxin removal when other water constituents are present, is an important research question to address. MC-LR is a deadly algal toxin released mainly by a most prominent cyanobacteria: *Microcystis Aeruginosa* in water ecosystems. Lake Erie has repeatedly hit the headlines in recent years due to large outbreaks of harmful algal blooms (HABs). The extent of pollution prompted the DWTPs across the lake basin to rethink about the existing treatment facilities.

In past, the bioaugmentation of specific bacteria had shown enhanced MC-LR removal [10,11]. However, these studies did not reveal the filter performance when other water pollutants co-occurred along with MC-LR. Owing to the antibacterial property of GO and rGO and concept of biofilter, these materials were first bio-optimized for their coating dose at which they showed at least 60% survivability rate of the MC-LR-degraders potent in forming biofilm. In the current study, to hypothesize the surface charge influence on the MC-LR removal (as it bears negative charge for the wider pH range: 3.5–10.4), a more electropositive surface was proposed. To achieve this, iron oxide was coated over the sand (IOCS or Fe filter) owing to a high pZC (>7.5) of the former than the latter (pH: 3–4) [12]. Submicron carbon particles (in form of graphene oxide) owing to their high adsorption capacity was also introduced in the above hypothesis to further investigate any rise in the adsorption performance of water pollutants, especially MC-LR, when coated on the electropositive surface (Fe sand) in form of FeGO filter media (Fe + GO). It should be noted that Fe + rGO was not considered as an option in this study, due to unsuccessful coating over the sand surface despite showing high electropositive surface of rGO particles (-14.3 ± 3.5 mV) when compared with GO particles (-37.5 ± 6.8 mV). Thus, in total, five filters were tested for the above presented problems and hypothesis including one control: uncoated sand media.

To the best of authors knowledge, this is the first time that an iron oxide-coated sand filter (herein after referred to as Fe filter), GO-coated filter (GO filter), and rGO-coated filter (rGO filter), are tested for their adsorption and biodegradation behavior of any cyanotoxin (MC-LR), in conjunction with MC-LR-degraders. To mimic a real treatment scenario, native bacterial species isolated from the filtration unit of a DWTP were co-cultured along with the MC-LR-degraders to study the overall biodegradation of MC-LR and other water pollutants. Additionally, the FeGO sand media was synthesized for the first time and tested for the removal of any water pollutant.

2. Material and methods

2.1. Chemicals and reagents

Microcystin-LR (MC-LR) was bought from Cayman Chemicals (Ann Arbor, Michigan, MI, USA) and a stock solution of 50 µg/mL was made by diluting 100 µg lyophilized film of MC-LR (as provided by the supplier) using 2 mL of HPLC-grade methanol and stored at −20 °C. Crystal violet and 3-(4, 5-dimethylthiazol-2-yl)-2,5-diphenyltetrazolium bromide (MTT) were purchased from Sigma Aldrich, (Ontario, Canada). Quartz sand was obtained from the filtration unit of the drinking water treatment plant (DWTP) from Chemin Ste-Foy DWTP, Quebec City, Canada.

Arthorobacter ramosus (NRRL B-3159) and *Bacillus* sp. (NRRL B-14393) were purchased from NRRL Agricultural Research Service (ARS) culture collection. All the analytical reagents used in preparing nutrient and culture media, LC-MS grade solvents and reagents used to prepare analytical mobile phases, were purchased from Fisher Scientific, (Ontario, Canada).

2.2. Synthesis of graphene oxide and reduced graphene oxide

Around 6 gm of graphite flake (mesh size 10) was mixed with 160 mL of concentrated sulphuric acid. To avoid explosive reaction, 15 mL of orthophosphoric acid was used along with 3 gm of NaNO₃. After 2 h of reaction, 20 gm of potassium permanganate was added to further oxidize the reaction. The reaction was left for 4–6 h. Soon after, 75 mL of distilled water was added very slowly and carefully (highly exothermic reaction) into the reaction mixture followed by a quick addition of 350 mL of distilled water. The reaction was stirred for half an hour and then 15–20 mL of 30% hydrogen peroxide was added to terminate the reaction. The reaction mixture was centrifuged at $5000 \times g$ for 30 min at room temperature to obtain the solid pellets which were later washed with distilled solution until neutral. The neutral washed solution was dried at 60 ± 3 °C overnight to obtain solid graphite oxide. For graphene oxide, various batches of 50 mg of graphite oxide were mixed with 100 mL distilled water and sonicated for 4 h until a uniform dispersion was obtained. The obtained mixture was dried at 60 ± 3 °C overnight to obtain solid graphene oxide (GO). The particle size distribution of GO showed a mean size of 298 nm.

To synthesize reduced graphene oxide in various batches, around 300 mg of ascorbic acid was added to 100 mL of graphene oxide (concentration: 0.5 mg/mL). The solution was stirred for three time periods viz. 20 mins, 40 mins and 70 mins. The solution pH was alkaline (pH 10.5) to keep the material stable via electrostatic repulsion. The temperature of the set-up was maintained between 60 and 70 °C. The obtained mixture was then dried at 60 ± 3 °C overnight to obtain solid reduced graphene oxide (rGO). Based on the material characterization results, single time period among the above three (reduction process time of 40 min) was chosen. The particle size distribution of rGO showed a mean size of 193 nm.

2.3. Bacterial survival test for the synthesized rGO and GO: Optimization study

From a stock solution of prepared GO solution (3330 mg/L), concentrations of 100 mg/L, 300 mg/L, 400 mg/L, 540 mg/L and 620 mg/L of GO were prepared in different Erlenmeyer flasks containing 10 mL of Luria Bertani media (supplementary section: Fig. S1). One flask without GO served as the negative control. After eight hours of incubation at 150 rpm at 30 ± 1 °C (16 times more than generation time), cell enumeration was reported based on the survival % for both MC-LR-degraders at various GO concentrations (as mentioned above). Cell enumeration obtained for the control case was assigned a 100% survival rate value. Each flask was inoculated with 4×10^7 cells/mL of respective MC-LR-degraders. A subjected minimum of 60% survivability value was chosen as the criterion for selecting the optimum dose in order to justify for the GO/rGO coated surface favoring the biofilm formation. The average of three plate counts was reported. (triplicate). However, the above experiment was performed under dynamic conditon (shaking incubator) as compared to the actual biofilter operation (static/fix bed system) where rGO/GO-coated sand are the filter adsorbents. Hence, the relationship to estimate the real GO/rGO dose per gram sand was balanced based on the static-dynamic non-experimental factor as explained in the supplementary section (Fig. S2). This helped in not overestimating the rGO/GO dose during sand coating. For the rGO material also, the same experimental method was executed as discussed above and survivability % was reported for each dose concentration.

2.4. Synthesis of GO-coated, rGO-coated, Iron oxide-coated (Fe) and FeGO-coated sand

According to the static-dynamic relationship, the real dose of GO and rGO with respect to the survivability rate was found to be 5 mg GO/gm-sand and 6.5 mg rGO/gm-sand, respectively. To effectively

coat GO and rGO over sand (individually), distilled water and ethylene glycerol was chosen, respectively as the base solution to get a uniform dispersion (screened based on 5 different polar solvents tested) after sonication. For coating, the dispersed solution (100 mL of GO/rGO per 100-gm sand) was mixed well with sand and later calcinated at 400 °C for about 4 h in a muffle furnace. The coated material was left to dry at room temperature overnight followed by activation using 0.1 M sulphuric acid for 30 min, neutralized and dried again before using it as the filter media.

Iron oxide-coated sand (Fe-sand) was synthesized to understand the change in the adsorption behavior of WQPs when Fe-sand was formulated with GO (FeGO). To coat iron oxide over the sand, crystalline ferric nitrate was chosen as the iron oxide source and was prepared according to the method described by Hansen et al. (2001) [13]. For FeGO-sand coating, GO at the concentration of 5 mg/gm of Fe-sand was chosen and was calcinated at 400 °C for 4 h and similar protocol for activation and drying was followed as mentioned above for GO/rGO.

2.5. Characterization of the synthesized submicron carbon materials and coated sand grains

Scanning electron micrographs (SEM) of the synthesized GO/rGO and prepared coated sand materials were recorded using Zeiss Evo®50 Smart SEM system between 5 and 15 kV. Also, the Fourier-Transform Infrared Spectroscopy (FTIR) data were recorded using a Perkin Elmer, Spectrum RXI, FT-IR instrument fitted with a lithium tantalate (LiTaO$_3$) detector. Energy dispersive X-ray (EDX) analysis was performed for confirming the atomic percentage of oxygen and carbon atoms in the synthesized GO/rGO and to determine the proportion of iron, carbon and oxygen in the Fe and FeGO coated sand surface. The zeta potential of the obtained coated grains was compared with the uncoated sand grains to report the degree of relative (as compared to uncoated sand grain) electro-positive surface obtained after the coating process. Pulverized sand grains (coated and uncoated) were suspended using ultrapure water in DTS1060 disposable cells, used as the zeta potential cells for Malvern Instruments according to the manufacturer instructions.

2.6. Screening the MC-LR-degraders for different sand composite

For screening the most potent MC-LR-degrader among *Arthrobacter ramosus* (A) and *Bacillus* sp. (B), a unique experimental set-up was prepared as mentioned in our previous work [3]. The set-up diagram is provided in the supplementary section (Fig. S3). For this, two sets of model reactor (10 gm coated sand, fixed size: 300 μm for each A and B) were placed horizontally as shown in Fig. S3. To inoculate the coated sand media, the influent solution of A and B was separately discharged through them at an intermittent rate of 30 mL (6×10^7 cells/mL) every 4 h (using an auto-dosage pump) to allow enough time for the biocells to proliferate in between two discharges. The cells were harvested in Luria-Bertani media and was centrifuged at $9000 \times g$ at room temperature to obtain the pellets which was mixed with lake water (Lake Sainte-Anne, (47.262879 N, −71.665158 W)) to obtain the discharge inoculum solution as mentioned above. As a control, uncoated sand media was also kept in the experimental set-up for comparison purposes.

The process was continued for 8 days and a sample was taken every 1-day, 4-day, 6-day and 8-day. For this purpose, a small amount of the material (~0.1 g for all cases) was taken from the top surface (as more biofilm is expected in this zone) and was suspended very quickly in 1.5 mL saline-buffer prepared in tap water to hydrate the living biocells (attached to sand). The sample was vortexed for 2 min at high speed to detach the biocells from the sand grains. The supernatant consisting of biomass and live cells were analyzed for the Crystal Violet (CV) assay and MTT assay, respectively, as per the protocol mentioned in our previous study [3]. The CV assay quantified the degree of biomass (live + dead cells) in a biofilm whereas the MTT assay quantified the live cells in the biofilm. The results were compared with the negative control (uncoated sand media). Flow rate was also estimated to indirectly determine the rate of biomass formation within the sand grains.

2.7. Column experiment and setup details

Fig. 1 shows the schematic representation of the filter set-up used for the experiment (actual set-up figure: supplementary Fig. S4
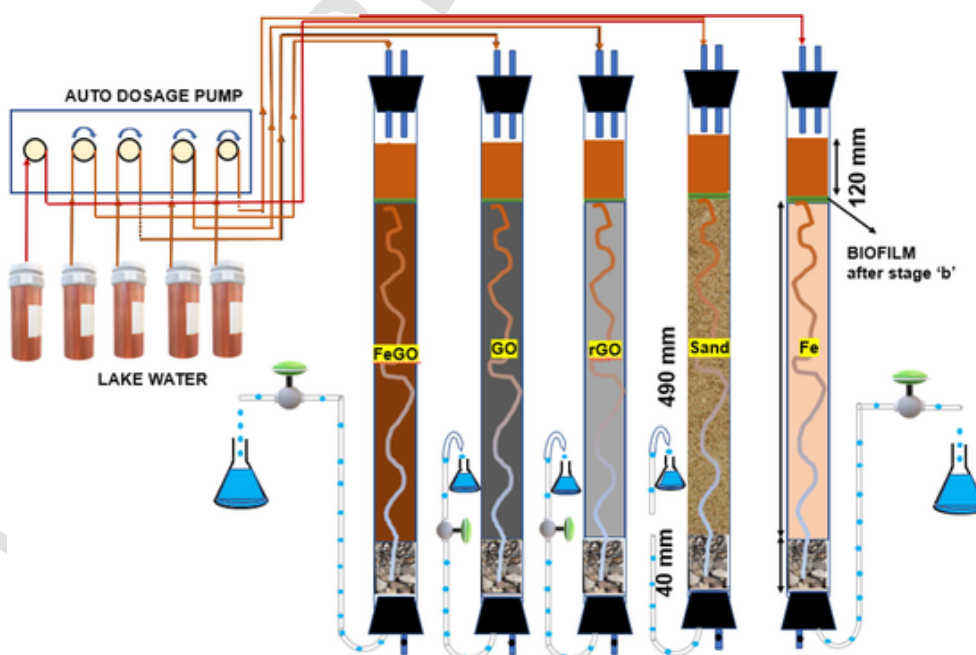

Fig. 1. Schematic representation of the column experiment using five filter media (rGO: reduced graphene oxide, GO: Graphene oxide, FeGO: Iron coated on graphene oxide coated sand, Fe: Iron coated sand).

(a)). The cylindrical glass rods of height 650 mm with an inner diameter of 20 mm and thickness of 1.5 mm were used for the column study. Around 490 mm of adsorbent media (coefficient of uniformity: 2.32) was put inside the dried column underlain by the drainage section (120 mm length) which comprised larger sand grains (4–8 mm size). The adsorbent media comprised of mixture of various sand grain sizes (range 125 μm-1000 μm) that eventually characterized the overall media for an effective diameter (D_{10}) of 210 μm. The grain size distribution curve is provided in the supplementary section (Fig. S4 (b)).

The column experiment was run for 3 stages. A) Stage 1: Physical adsorption studies of water quality parameters including MC-LR removal for 5 weeks (1 week = 1 cycle). B) Stage 2: Biofilm formation phase, wherein the column was fed intermittently using an auto-dosage pump with lake water. The lake water was inoculated (9×10^8 cells/mL) with the screened MC-LR-degrader for the respective adsorbing filter media, co-cultured with the native bacterial cells isolated from the filtration unit of the DWTP (discussed in detail in next section). Every hour, 40 mL per intermittent discharge was carried out using an auto-dosage pump. Stage 2 filter operation was continued for a total of 11 days until conclusive evidence of substantial biofilm formation was reported (detail in Section 3.5), C) Stage 3: Biodegradation phase study of water quality parameters for 6 weeks. For the daytime hours (10 am to 6 pm), the filters were operated every hour and during night hours, the auto-dose pump was set to run every 4 h where sampling for the WQPs was done at 2 pm every 2nd and 5th day of a 7-day cycle. For stage 1 and stage 3 filter operation, water pollutant-spiked lake water (details in Section 2.9) was discharged intermittently every hour (40 mL volume) for the analysis of various water quality parameters viz, total coliform removal, total turbidity removal, dissolved oxygen, metal removal (copper and iron), flow rate, conductivity, pH, TOC removal and ammonia removal. The details of the initial concentration of these WQPs are mentioned in Section 2.9.

2.8. Biofilm characterization for the stage 2 filter operation

Before the onset of stage 3 filter operation, a healthy biofilm formation was a pre-requisite to understand the effect of inoculation (bioaugmentation) on MC-LR removal. Each filter column was inoculated using the screened MC-LR-degraders for respective sand composite (Section 3.4) along with the native bacterial cells isolated from the DWTP [14]. This co-culturing aspect of MC-LR-degrader with the native bacterial community (combination of *Chryseobacterium* sp. and *Pseudomonas fragi* = named 'X', from here on) was proven to accelerate the MC-LR biodegradation [3]. Also, considering the real scenario of the filtration unit in the DWTP and for the improvement of MC-LR biodegradation, co-culture practice seemed more rational. A total cell concentration of 6×10^7 cells/mL (as mentioned before) was inoculated where each bacterial species was divided equally (2×10^7 cells/mL each). The columns were fed every 6 h with the inoculum and given enough time between the next discharge for the biocells to adhere to the sand composite and proliferate. Every 3 days, for 12 days, sampling for the biofilm quantification was done in a similar manner (CV assay, MTT assay) as discussed in Section 2.6.

2.9. Analysis of water quality parameters (WQPs)

2.9.1. pH, dissolved oxygen and conductivity

During the filter operation, change in pH and DO value for the influent/effluent indicated the activity of biofilm formation and water quality. The effluent (or filtered) water was duly checked for DO value measured using a portable F4-Standard probe (Mettler Toledo Inc), to check for any anoxic environment built-up in the drainage zone of the column (<2 mg/L-O_2). Also, the pH information was important to understand the degree of alkalinity that is needed to maintain for the next treatment step, i.e., disinfection, if the results are to be applied. The conductivity of the sample was measured using a Met-

tler Toledo™ S230 SevenCompact™ Conductivity Meter. The change in conductivity was primarily used to test for any micro-leaching phenomenon that had happened from the coated sand.

2.9.2. Dissolved organic carbon, ammonia, nitrite, nitrate, iron, copper, magnesium removal

In general, the primary objective of the filter unit is to remove the organic matter from the source water. Hence, in this study, the DOC removal study was done where the initial DOC of the lake water was found to be around 6 ± 0.9 mg/L. All the measurements were done using a Shimadzu 5000A analyzer (Shimadzu, Japan). In brief, around 30 mL of the effluent sample was filtered using a 0.45 μm glass-fiber filter and analyzed for the DOC.

Ammonia-N, nitrate-N and nitrite-N removal studies was performed by spiking ammonium sulfate, sodium nitrate and sodium nitrite, respectively, in the lake water matrix to reach an initial concentration of 5 ppm, 10 ppm and 50 ppm of NH_4-N, NO^{2-} and NO^{3-}, respectively. Initial ammonia-N, nitrite-N and nitrate-N concentration in the lake water was determined to be 1.3 mg/L, 2.1 mg/L, and 0.5 mg/L, respectively, and the spiking was done accordingly. The analysis was done by a similar method as discussed in [3].

To evaluate the filter performance for the removal of metal ions, Fe^{2+} and Cu^{2+} was chosen as the metal indicators in lake water where $FeSO_4 \cdot 7H_2O$, $CuSO_4 \cdot 5H_2O$ was used as the metal source to spike it (stoichiometric equivalent) at an initial concentration of 10 ppm and 20 ppm respectively. When copper test was reported, it was made sure that there was no ammonia (spiked) in the water and vice-versa, because of the likely interference of these compounds to form a complex with each other, thereby incurring overestimation in reporting the ammonia/Cu^{2+} removal. The detailed method for estimating copper and iron are mentioned in Mehlig et al. (1941) [15] and Fortune et al. (1938) [16], respectively.

2.9.3. Turbidity, total Coliform, specific UV254 removal

Initial turbidity of the lake water was around 13.2 ± 4 NTU. All the filters were tested for their efficiency in removing suspended particles from the lake water using HACH instrument 2100 model where the effluent turbidity was reported in Nephelometric Turbidity Unit (NTU).

Total coliform removal test was performed twice a cycle (every 2nd and 5th day of the week or cycle) for the filtered water sample by membrane filtration technique according to a standard method [17]. Initial total coliform present in the lake water was determined to be 56 CFU $\pm$ 14/100 mL. To report the degree of natural organic matter removal, an indirect measurement using specific UV254 (SUVA) was done, where the change in SUVA for the influent and effluent was reported for the organic matter removal.

2.9.4. Flow rate and MC-LR removal

The flow rate for each filter was reported in m/h ($m^3/m^2/h$) after the end of each cycle. A stagnant water head of 70 ± 5 mm was maintained (from top layer of sand composite media) throughout the measurement process. The flow rate for any filter should not decrease to 1/4th of the initial flow rate during any stage of the biofilter operation which was kept as the subjective minimum criterion. If the flow falls below 1/4th the initial flow rate value, backwashing was performed for the filter at a flow rate low enough to not fluidize the bed and should not cause $>15\%$ bed expansion.

MC-LR from the stock solution was diluted appropriately to the lake water (lake water had no detectable MC-LR) to obtain an influent MC-LR concentration of 50 μg/L. The effluent was analyzed for MC-LR twice a cycle (or week) using a method adapted from Roy-Lachapelle et al. (2019) [18]. Briefly, a 20-μL sample aliquot was analyzed by ultra-high-performance liquid chromatography coupled to high-resolution mass spectrometry (Thermo Q-Exactive Orbitrap) through a positive electrospray ionization source. The chromatographic column was a Thermo Hypersil Gold with C18 selectivity (100×2.1 mm, 1.9 μ

m particle size). MC-LR was detected in full-scan MS mode (resolution set at 70,000 FWHM at 200 m/z) and quantified against a matrix-matched lake water calibration curve [18]. The analytical method was validated for linearity, accuracy, and precision; the performance was compliant with acceptance criteria [18]. The method limit of quantification (LOQ) was set at the lowest concentration level of the calibration curve (i.e. 0.1 µg/L). At the end of stage 2 and stage 3 filter operation, all the filters were subjected to three different MC-LR influent concentration of 5 µg/L, 20 µg/L and 50 µg/L to better understand the limitation of each filters.

2.10. Regeneration and reuse studies

A regeneration and reusability study for all the filter media was performed to understand the behavior of adsorption and to envisage the economic feasibility of using each filter medium. The adsorbate used for the study was Rhodamine-B dye which represented the colored and model contaminant. The dye-adsorbate was used at an initial concentration (C_o has an optical density of 0.21) of 1 mg/L for each adsorbent. A continuous flow rate of 4 mL/min was maintained using a peristaltic pump and the effluent OD at 550 nm (C_e) was taken after every bed volume (25 mL) to estimate the adsorption of dye material on to the sand composites. A column height of 7.5 cm for each adsorbent was used (set-up shown in the supplementary section: Fig. S5). The breakthrough period was determined at $C/C_o = 0.05$) for each of the sand composites. After the exhaustion of bed material ($C/C_o \sim 1$), the adsorbent media was regenerated using acetone solution and was reused again for the dye-adsorption study. The saturation adsorption capacity (Wsat) of the bed media was reported for each filter media for 3 regenerated cycles to understand the reusability aspect of each adsorbent. The following equation (Eq. 1) was used for calculating the Wsat (mg/g) value:

$$\text{Wsat} = (\int_0^t UoCo\left(1 - \frac{c}{c_0}\right))/(g - \text{adsorbent})$$

(1)

where, Uo is the flow velocity in L/minute, Co is the initial adsorbate concentration in mg/L and t is the breakthrough time in minutes.

2.11. Statistical analysis and graphics

All statistical analyses comprising standard deviation, average, student *t*-test, p-value comparison, Principal Component Analysis (PCA) and all graphical presentations were performed using the ORIGIN software (Version 8.5; OriginLab).

3. Results and discussion

3.1. Bacterial activity test for the synthesized rGO and GO

Table 1 shows the cell enumeration results of two MC-LR-degraders viz. *Arthrobacter ramosus* and *Bacillus* sp. for GO and rGO at various dose concentrations (mentioned in section 2.3). A high GO/rGO dose was required to provide high surface area for coated sand, hypothesizing better MC-LR adsorption on the coated surface and at least a 60% survivability of the MC-LR-degraders was also required to proceed with the screening experiment as the biofilm formation was a pre-requisite for biofilter operation. However, a high dose of GO/rGO was antibacterial (cell count decreased, Table 1) and thus the maximum dose was restricted to 640 mg/L.

It was observed that 400 mg/L of GO showed 62% and 61% survivability while 520 mg/L of rGO showed survivability of 62% and 64% for *Arthrobacter ramosus* and *Bacillus* sp., respectively. As the dose of GO and rGO was increased beyond 400 mg/L for GO and 540 mg/L for rGO, the survivability % also decreased and hence the above values, i.e., 400 mg/L and 520 mg/L for GO and rGO, were selected (dynamic value, section 2.3). To convert this dynamic value to static

Table 1

Cell-enumeration to study the survivability rate of Microcystin-LR-degraders under different concentrations of Graphene Oxide and reduced Graphene Oxide.

Case	*Arthrobacter ramosus*#	% survival	*Bacillus* sp.#	% survival
Zero	32 ± 7	100	51 ± 12	100
100 mg/L GO	28 ± 5	87	42 ± 13	82
300 mg/L GO	25 ± 8	78	36 ± 8	71
400 mg/L GO	20 ± 3	62	31 ± 9	61
520 mg/L GO	14 ± 6	44	18 ± 6	35
640 mg/L GO	12 ± 9	38	14 ± 4	27
Case	*Arthrobacter ramosus*#	% survival	*Bacillus* sp.#	% survival
Zero	32 ± 6	100	51 ± 6	100
100 mg/L rGO	29 ± 2	92	48 ± 2	94
300 mg/L rGO	24 ± 7	81	41 ± 7	80
400 mg/L rGO	22 ± 8	75	37 ± 6	73
520 mg/L rGO	19 ± 4	62	33 ± 3	64
640 mg/L rGO	16 ± 6	51	18 ± 5	35

The count of bacterial colonies was done based on the 10^5 dilution LB-media agar plates ((rGO: reduced graphene oxide, GO: Graphene oxide, FeGO: Iron coated on graphene oxide coated sand, Fe: Iron coated sand).

value, 5 mg/g-sand and 6.5 mg/g-sand was chosen as the coating dose for GO and rGO, respectively. The rationale for the static-dynamic calculation is shown in the supplementary section (Fig. S2).

3.2. Characterization of the synthesized materials: GO/rGO

To characterize the obtained graphene oxide, an FT-IR interferogram was generated and analyzed for the presence of the oxygen-functionalized groups to validate the oxygen atoms intrusion in the synthesized graphene oxide. Fig. 2 (A) shows the FT-IR spectra for the graphite flake and graphite oxide. From the FT-IR, spectra, –COOH, –OH and C-O-C groups were completely absent for the graphite flake while these groups were observed at the characteristic wavenumbers: 1719 cm^{-1}, 3200 cm^{-1} and 1351–1390 cm^{-1}, respectively for graphite oxide. The FT-IR spectra also showed the evidence of skeletal vibration of the graphene plane at a wave number of around 1560 cm^{-1}. This suggested that the exfoliation of the graphite oxide happened in the form of graphene oxide. Fig. 2 (B) shows the FT-IR spectra for the graphene oxide prepared at three different pH: 3, 7 and 10.

Fig. 3 (A) shows the SEM images of the graphite flake and synthesized GO at pH 3, 7 and 10. Skeleton vibration of the graphene plane which occurs at the characteristic peak of 1560 cm^{-1}, was chosen as the main criterion to distinguish the degree of exfoliation in graphene oxide. It was observed from the FT-IR spectra that the peaks were more pronounced for the graphene oxide at pH 10. Also, the SEM demonstrated that the synthesized GO showed more exfoliation on its surface under alkaline conditions.

To further validate the synthesis of graphene oxide, EDX analysis was carried out to determine the ratio of C/O in terms of the atomic percentages. EDX spectra showed that the ratio of C/O for graphite flake was >75 while it reduced to 2.1 due to the oxidation of graphite into graphite oxide. Sonication of graphite oxide to graphene oxide at different pH increased the C/O ratio to 2.5, 2.8 and 2.2 at pH of 10, 7 and 3, respectively. The minimum ratio among all was at pH 10 which attributed to more oxygen atom intrusion into the graphene sheet as compared to pH 3 and 7. Thus, for the sand thermal coating, the alkaline environment was chosen for dispersing the GO compound. To characterize the rGO compound, FT-IR spectra were obtained (Figure
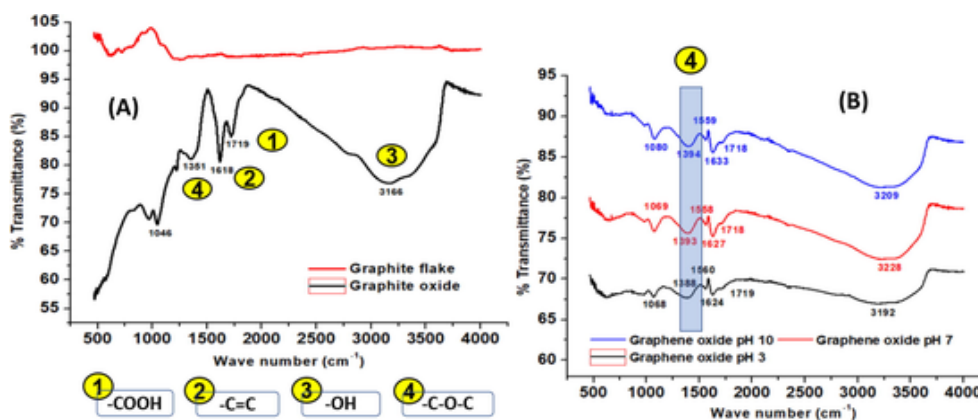
Fig. 2. FT-IR spectra for the A) graphite flake and synthesized graphite oxide, B) Graphene Oxide at different pH.
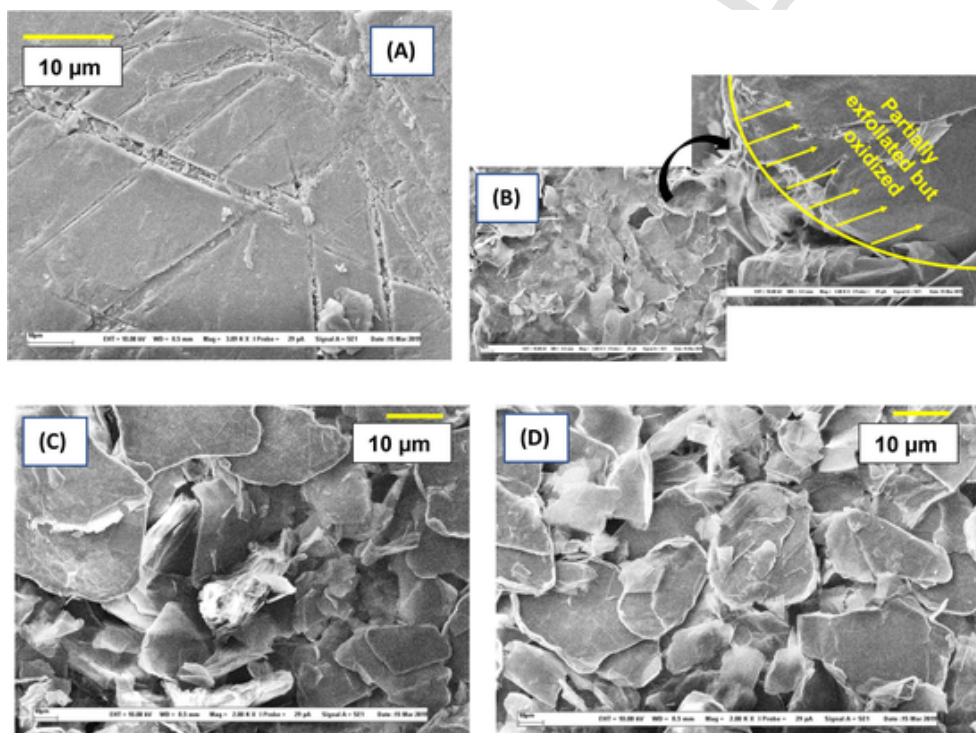

Fig. 3. SEM images of the A) graphite flake, Exfoliated graphene oxide at B) pH 3, c) pH 7 and D) pH 10.

in supplementary section: Fig. S6). It was observed that rGO after 40 min of reaction time (40 min reduction of GO) showed the maximum oxygen reduction (especially of the –OH peak at 3200–3300 cm^{-1}).

3.3. Characterization of the coated sand composite

Table 2 shows the EDX analysis for all the synthesized filter media. A high percentage of carbon was found to be coated in GO ($\sim$70%) and FeGO (52%) coated-sand grains whereas, maximum atomic Fe % of 43% and 6% was found for the iron-coated grains viz. Fe and FeGO, respectively. This ensured high iron oxide coating in the case of Fe grains, while a balance of carbon and iron oxide for FeGO grains. According to the atomic percentage values (Table 1) the chemical formula obtained for Fe and FeGO sand grains was $SiFe_{18}O_{22.5}$ and $SiFe_{7.5}C_5O_8$, respectively. The surface zeta potential measured for Fe, FeGO, GO and rGO was -21.3 mV, -13.4 mV, -22.3 mV and -18.7 mV, respectively. As compared to the zeta potential of an uncoated sand grain, all the surfaces were found to be more electropositive, especially the Fe grain.

3.4. Screening the MC-LR-degraders for each sand composite

Fig. 4 (A) and (B) present the bar chart graphs for the CV assay and MTT assay, respectively for all the sand composite adsorbents. For rGO and FeGO, *Arthrobacter ramosus* (AR) showed higher optical density than *Bacillus* sp. (BS), for both CV as well as MTT assay. The observed mean difference for rGO and FeGO between the data set for AR and BS was 0.19/0.24 and 0.84/0.32 for CV and MTT assay, respectively. For GO and Fe, the OD value between AR and BS data set was similar. The p-value of 0.11 was obtained for GO case (CV assay data sets for AR and BS) and 0.15 for Fe case (CV assay). The mean difference of OD between AR and BS for CV and MTT assay was -0.11 and 0.06, respectively. Hence, AR and BS seemed the most appropriate choice for GO and Fe, respectively. For sand, as can be observed, BS was the preferred choice over AR.

Table 2
EDX analysis for all the synthesized filter media.

Filter Media	Atomic% C	Atomic% O	Atomic% Si	Atomic% Fe	Color	Figure	Zeta potential (mV)
Iron oxide coated sand (Fe)	NA	53.97	2.40	43.05	Orange		−21.3
FeGO (Fe + GO)	22.4	36.93	4.60	34.5	Brownish black		−13.4
GO	69.87	24.56	4.87	NA	Black		−22.3
rGO	84.91	13.76	< 1	NA	Light black		−18.7
Sand	0.00	72.30	26.70	NA	Yellowish white		−43.2

(rGO: reduced graphene oxide, GO: Graphene oxide, FeGO: Iron coated on graphene oxide coated sand, Fe: Iron coated sand).
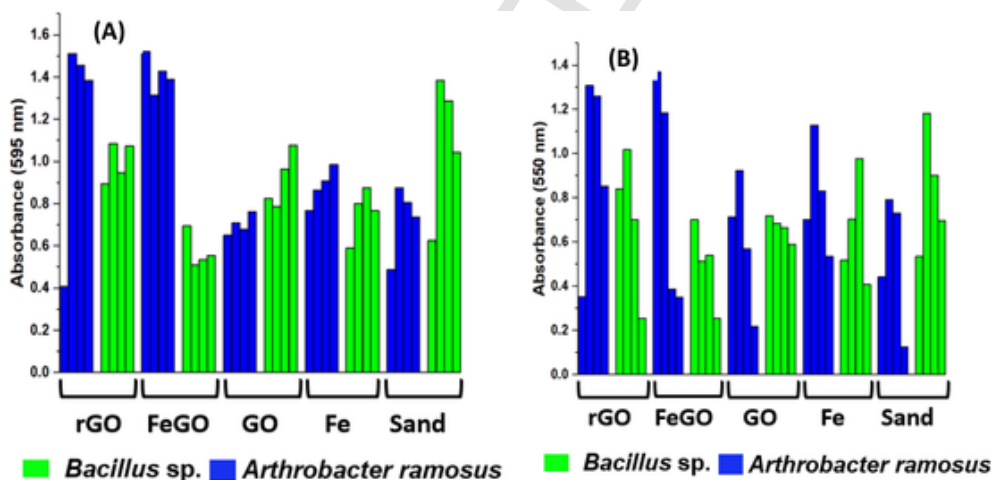
Fig. 4. Biofilm screening test for all the synthesized filter media quantified as A) CV assay and B) MTT assay (rGO: reduced graphene oxide, GO: Graphene oxide, FeGO: Iron coated on graphene oxide coated sand, Fe: Iron coated sand).

3.5. Biofilm formation study: Stage 2 filter operation

After the stage 1 filter operation, each filter was inoculated with their respective screened MC-LR-degraders (along with native bacterial co-culture: 'X' as mentioned in Section 2.8). Fig. 5 (A), (B) and (C) represent the CV assay, MTT assay and flow rate (m/h) for each filter. All filters showed an increase in biomass production especially for the sand surface (uncoated) as compared to other sand composite materials (average CV assay OD of 0.78 as compared to the next best OD of 0.59 for rGO). The rGO/GO coated-sand material still showed better biomass formation (average CV assay OD of 0.59/0.51) on its surfaces as compared to Fe and FeGO sand composites (average CV assay OD of 0.26/

0.36). The choice of the 60% survivability principle corresponds well with the biomass growth. This can also be perceived from the MTT assay result too (Fig. 4 (B)) where it can be observed that the biofilm adhered to rGO/GO sand composites (average MTT assay OD of 0.43/0.36) surface had better cell viability only next to the uncoated sand surface (average MTT assay OD of 0.49).

The flow rate for all the filter decreased as was expected because of the tortuosity resistance in flow due to the biomass formation between the sand grains. The maximum decrease in the flow rate was measured for the sand filter (43%) followed by rGO (36%) and GO (33%) coated sand filter. These results go in coordination with the biofilm formation for both CV as well as MTT assay (all showed a correlation of ~−0.9, correlation table not shown).
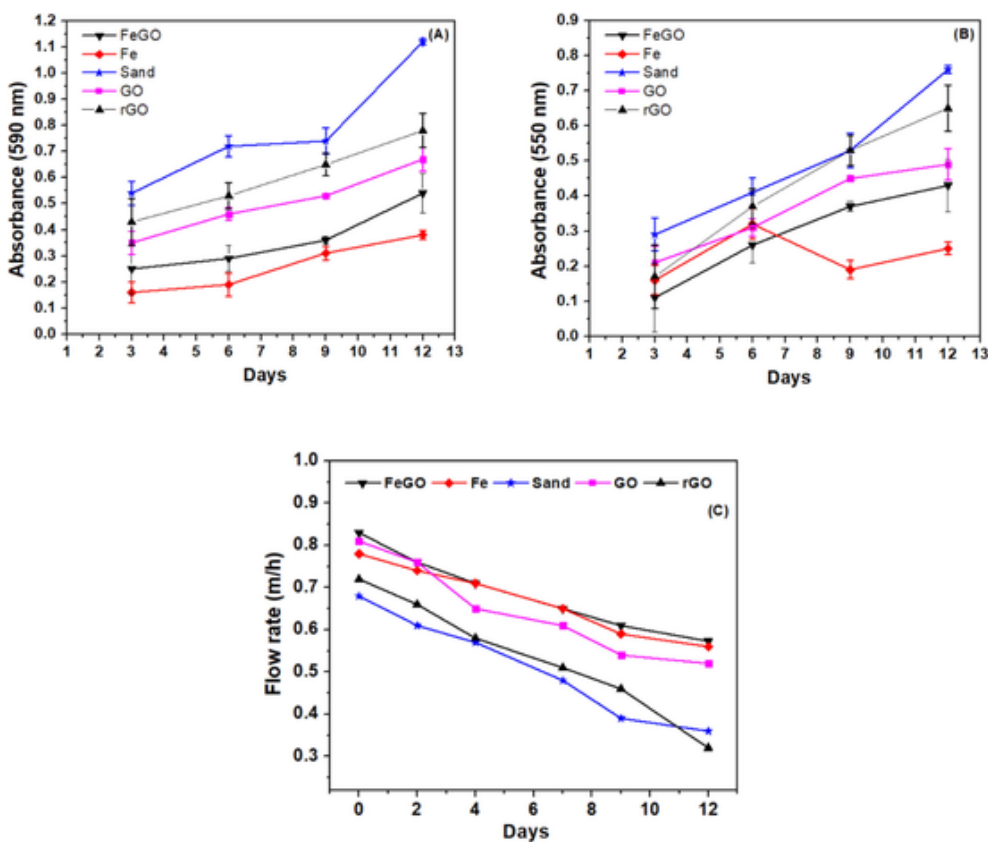
Fig. 5. Biofilm forming phase study for A) biomass formation (CV assay), B) cell viability (MTT assay) and C) Flow rate (m/h) (rGO: reduced graphene oxide, GO: Graphene oxide, FeGO: Iron coated on graphene oxide coated sand, Fe: Iron coated sand).

3.6. Water quality parameters (WQPs)

Table 3 presents various WQPs for all the sand composite media comprising both the phases of filter operation. Maximum NH_4-N removal was observed for the FeGO filter (56%) in both the stages where bioaugmentation improved the removal efficiency by 12% (44% to 56%) whereas the GO filter showed the maximum improvement of 24%. The second-best filter for ammonia removal was the Fe filter which showed removal of 46% in stage 3 indicating that it was iron more than GO that was responsible for high ammonia adsorption in the case of FeGO. In contrast, for the oxidized form of nitrogen, i.e., nitrate, FeGO was the third-best filter that showed 45% removal next to the rGO/GO filter (each showed over 60% nitrate removal). The Fe filter was the least effective with just over 12% removal indicating the contrasting nature of iron for ammonia and nitrate adsorption.

Maximum average total coliform removal of over 80% was observed for the GO and rGO filters followed by 68%, 47%, and 14% for the FeGO, Fe and sand filters, respectively. This indicated that GO mixed with Fe (for the FeGO filter) enhanced the total coliform removal by 21%. The GO surface might have created a physical disruption of the bacterial cells or created an oxidative stress environment for the coliforms [19]. Bioaugmentation of MC-LR degraders and native bacterial species did not enhance the total coliform removal by much (maximum of 9% in the rGO filter) which clearly illustrates that the predation mechanism was not prevalent in these biofilters [20]. Hence, modification of the sand directly affected coliform removal by other mechanisms such as trapping, oxidative stress, or physical disruption as mentioned above.

The maximum DOC removal of 62% each were obtained for the GO and rGO filters whereas the Fe and sand filters performed worst with just 23% and 17%, respectively. DOC removal enhanced maxi-

mally during the biodegradation phase (stage 3) for the rGO filter (50%) followed by the GO filter (26%). The highest DOC removal by the GO filter can mainly be attributed to enhanced hydrophilicity of the sand surface due to the GO coating leading to more interaction with the chemical contaminant in aqueous media (here lake water) at the nanometer level [21]. After long usage of the GO filter (13 weeks including all the stages), there was no evidence of any surface peel-off or leaching. Hydrogen bonding and π–π interaction could also be held responsible for high DOC removal/adsorption on GO-coated sand media [9].

Maximum copper removal was observed for FeGO (71%) followed by 54% and 58% for the rGO and GO filters, respectively as compared to < 25% for the sand filter and 40% for the iron-coated sand filter. On the other hand, FeGO, GO and rGO showed > 95% Fe^{2+} ions removal for both stage 1 and 3 of filter operation whereas the sand filter and the iron-coated sand filter showed < 50% adsorption. High adsorption of metal ions (copper and iron) for FeGO can be linked to low pH effluent among all the filters (Table 3). This removal mechanism involves the leaching of H^+ ions when the already sorbed-metal surface is exposed to the cationic metal ions [22]. However, a possible desorption mechanism occurs when the sorbed-surface becomes alkaline and meets the diffused H^+ ions to release back the sorbed metal ions. Hence, any alkaline pretreatment of raw water before filtration may make these filters less efficient. On the other hand, high metal adsorption can be linked to the multi-layered and rough surface GO coating over the planar sand surface (SEM image, refer Fig. S9) which allowed more adsorption of metal ions. Gao et al. (2011) [23] suggested a core–shell structure of GO that formed over the sand surface responsible for 5-times more Hg^{2+} ions adsorption as compared to sand media. Also, in the above study, the coating of GO per gram of sand was quite close (3.5 mg/g-sand) to the present study (5 mg/g-sand) and hence intergranular diffusion resistance can be accounted almost similar

Table 3
Water Quality Parameters (WQPs) for all the filter media tabulated in the form of their concentration present in the filtered sample for both the stages of filter operation.

Water Quality Parameter	Stage	FeGO	Fe	Sand	GO	rGO
Conductivity	Stage 1	107 ± 16	110 ± 14	90 ± 32	212 ± 12	209 ± 23
	Stage 3	114 ± 13	116 ± 12	87 ± 17	211 ± 32	232 ± 21
DO (mg/L) [5.7 mg-O_2/L]	Stage 1	5.31 ± 0.34	5.48 ± 0.13	5.2 ± 0.40	5.6 ± 0.32	5.4 ± 0.17
	Stage 3	4.56 ± 0.18	4.43 ± 0.26	4.1 ± 0.22	4.7 ± 0.15	4.4 ± 0.32
Time to filter 40 mL standing water (min)	Stage 1	10.5 ± 1.5	9.1 ± 0.6	13.3 ± 1.7	10.76 ± 1.6	13.3 ± 2.9
	Stage 3	15.4 ± 1.2	13.3 ± 1.7	25.6 ± 2.7	13.7 ± 1.1	29.1 ± 3.3
NH_3-N (mg/L) [5 mg/L]	Stage 1	2.8 ± 0.5	3.1 ± 0.6	3.3 ± 0.7	4.2 ± 0.3	3.3 ± 0.4
	Stage 3	2.2 ± 0.2	2.7 ± 0.4	3.72 ± 0.6	3.0 ± 0.5	3.2 ± 0.5
NO_2^--N (mg/L) [10 mg/L]	Stage 1	7.8 ± 0.2	7.9 ± 0.8	6.2 ± 0.5	5.5 ± 0.6	6.1 ± 0.5
	Stage 3	7.5 ± 0.3	7.5 ± 0.8	5.8 ± 0.4	4.9 ± 0.4	5.8 ± 0.5
NO_3^--N (mg/L) [50 mg/L]	Stage 1	30.6 ± 1.9	44.4 ± 6	31.9 ± 4	20.9 ± 4.1	21.9 ± 4.3
	Stage 3	27.5 ± 2	43.7 ± 3	29.9 ± 4	19.76 ± 2	19.32 ± 3
pH	Stage 1	5.87 ± 0.3	6.17 ± 0.2	6.18 ± 0.4	5.99 ± 0.1	6.16 ± 0.1
	Stage 3	5.99 ± 0.1	6.11 ± 0.2	5.78 ± 0.4	5.76 ± 0.7	6.43 ± 0.3
Total Coliform (per 100 mL) [56 CFU]	Stage 1	17 ± 5	19 ± 4	47 ± 6	14 ± 3	16 ± 6
	Stage 3	16 ± 3	27 ± 4	44 ± 5	10 ± 2	11 ± 2
Turbidity (NTU) [13.2]	Stage 1	2.82 ± 0.39	3.55 ± 0.76	3.12 ± 0.16	1.34 ± 0.47	1.66 ± 0.28
	Stage 3	2.45 ± 0.38	3.44 ± 1.14	4.27 ± 0.35	1.28 ± 0.53	1.61 ± 0.41
Cu (mg/L) [20 mg/L]	Stage 1	6.2 ± 2.7	14.1 ± 2.3	15.4 ± 2.9	11.4 ± 3.1	13.1 ± 2.4
	Stage 3	5.9 ± 0.9	11.8 ± 1.4	15.7 ± 1.9	8.4 ± 3.3	9.2 ± 1.6
Fe (mg/L) [10 mg/L]	Stage 1	0.18 ± 0.14	6.3 ± 0.4	6.7 ± 1.43	0.18 ± 0.12	0.21 ± 0.12
	Stage 3	0.26 ± 0.15	6.2 ± 0.3	5.6 ± 0.70	0.34 ± 0.19	0.41 ± 0.32
MC-LR removal (%) [50 μg/L]	Stage 1	71.2 ± 8.1	1.15 ± 9.4	16.3 ± 20.3	79 ± 19.4	44.2 ± 10.6
	Stage 3	85.8 ± 11.7	33.5 ± 17	54.6 ± 14	82.5 ± 6.8	91.4 ± 6.5
DOC removal [6 mg/L]	Stage 1	3.7 ± 0.1	4.8 ± 0.2	4.6 ± 0.2	3.1 ± 0.3	4.4 ± 0.1
	Stage 3	3.4 ± 0.23	4.5 ± 0.1	4.8 ± 0.2	2.3 ± 0.4	2.2 ± 0.2

Initial concentration of each WQP is given in big bracket (rGO: reduced graphene oxide, GO: Graphene oxide, FeGO: Iron coated on graphene oxide coated sand, Fe: Iron coated sand).

that formed the basis for comparison of GO-coated sand in the former study that studied a commercialized filter media: activated carbon.

3.7. Understanding the water quality parameters (WQPs) removal using PCA and deciding the best filter

Fig. 6 (A) and (B) represents the PCA biplot graph for stage 1 and stage 3 filter operation. The biplots comprise of filters as the observation variables and various WQP (based on their removal %) as the main variables. Principal component 1 (PC1) and Principal component 2 (PC2) accounted for 57% and 29% of the total variation in data while its 66% and 25% for stage 1 PCA and stage 3 PCA, respectively.

Since PC1 showed a highly variable load in both the cases, hence, the loading scores obtained on PC1 axis were primarily used to determine the overall filter (observation variables) performance and their % improvement from stage 1 to stage 3. The overall best and worst loading score (LS) for stage 1 was −2.98 and +2.67 and for stage 3 it was −2.92 and +2.43, respectively. From the LS data, the best filter in stage 1 was GO (LS: +2.67) followed by rGO (LS: +1.58), FeGO (+0.70), Sand (LS: −1.97) and Fe (LS: −2.98). In stage 3 filter operation, the rank followed: rGO (+2.43) > GO (+2.20) > FeGO (+0.86) > Sand (@2.56) > Fe (−2.92). A major improvement (in terms of LS score) in the filter performance was observed for rGO (53%) after the biofilm formation, followed by sand (30%) and FeGO (23%). A high improvement for rGO was mainly contributed from
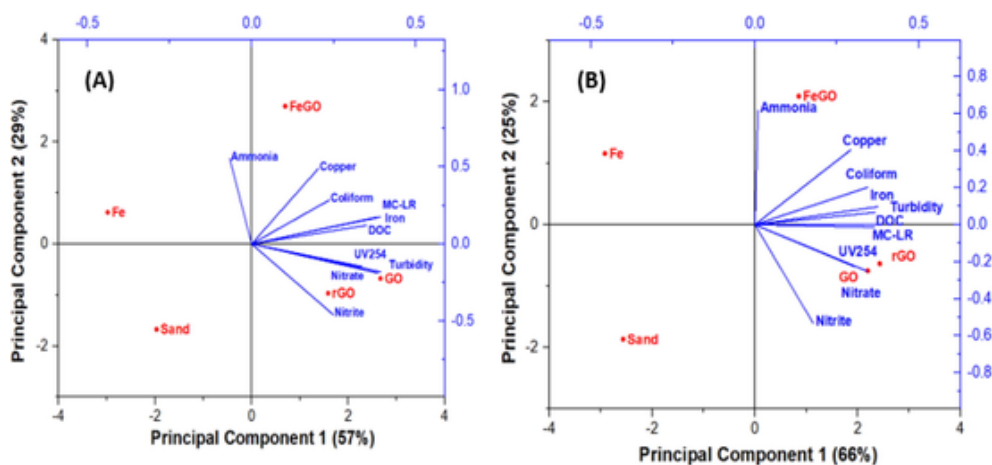
Fig. 6. Principal component analysis for water Quality Parameters (WQPs) as the main variables and the filters as observation variables: (A) Physical adsorption stage (stage 1), B) Bio-adsorption stage (stage 3). (rGO: reduced graphene oxide, GO: Graphene oxide, FeGO: Iron coated on graphene oxide coated sand, Fe: Iron coated sand).

the enhanced removal of copper, DOC and nitrite by 36%, 28% and 14%, respectively. The poor performance of the uncoated sand filter and Fe filters in both the stages (1 and 3) was evident from the PCA biplot which shows their position (red dot) in the far end 3rd and 2nd quadrant, respectively and no proximity with PC1 or eigenvectors of any WQPs. However, if an overall PCA biplot is investigated, there does not exist much difference between both the stages of the filter performance. Except for the ammonia eigenvector, all other WQP showed a positive correlation (>0.5) with MC-LR for both the filter operation stages (correlation matrix shown in the supplementary figure: Figs. S7, S8). The proximity of FeGO with the ammonia eigenvector was justified owing to its best ammonia removal performance (55%) as compared to other filters (especially uncoated sand: 25% only).

Copper was the closest eigenvector to ammonia and best related to the latter with a correlation factor of 0.64. This can be attributed to the complexation of the two compounds which lead to their removal simultaneously. In this study, there was no specific study done to analyze their complex and thus it would be interesting to study this parameter by the plant operator in DWTPs as it may lead to health problems in humans such as digestive problem, collapse and vomiting if detected in the treated water and is not removed.

3.8. Microcystin-LR removal

The average mean MC-LR removal for stage 1 was 71.2%, 1.15%, 16.3%, 79%, 44% for FeGO, Fe, Sand, GO and rGO, respectively. The poor removal efficiency of MC-LR in the Fe filter can be attributed to a planar surface morphology of Fe grains (refer to SEM image: supplementary section: Fig. S9). Despite a high electropositive surface (Table 1), Fe grains could not adsorb MC-LR molecules and performed below par even to the control filter. In contrast, the FeGO and GO filters performed quite well achieving >70% MC-LR removal which can mainly be due to roughness (functionalized groups of graphene oxide layers) on their surface as observed from the SEM images (Fig. S9). The functionalized groups containing more oxygen atoms could be the reason for making the surface more hydrophilic that might have allowed more surface attachment of the hydrolyzed MC-LR molecules [24].

On the other hand, a lower hydrophilic surface in the case of rGO-coated sand media (as compared to GO-coated sand), due to functionalized compounds containing fewer oxygen atoms, might be the reason for less MC-LR attachment (for physical adsorption phase). Also, the BET isotherm showed a high mesoporous surface with a specific surface area of 33.8 m^2/g for GO-coated sand as compared to 5.5 m^2/g for uncoated sand, respectively (BET isotherm is shown in supplementary section: Fig. S10). Teixidó et al. (2011) [25] too showed strong sorption (10^6 L/kg) of hydrophilic compounds (sulfamethazine) on the car-

bon surface (biochar) that mainly found electron donor–acceptor (EDA) interaction (due to ring structure in sulfamethazine) with π electron-rich graphene surface responsible for the adsorption. MC-LR consists of a benzene ring in the Adda group that can form the pi-pi interaction with the graphene surface. MC-LR consists of fraction of such EDA (ADDA group) in their whole macromolecule and thus such possibility of adsorption could likely be possible. Also, Coulombic attraction between negatively charged MC-LR and more electropositive charged surface of FeGO (−13.4 mV) and GO (−22.3 mV) sand media as compared to the uncoated-sand surface (−43 mV) could be held responsible for high MC-LR removal in case of GO and FeGO. However, the same theory does not hold for Fe and rGO sand grains, especially Fe which showed almost the same degree of electropositive surface (−21.3 mV) as GO-coated sand. Hence, the mesoporous surface layer of GO could be the main contributor to high MC-LR adsorption [26]. Apart from performing MC-LR analysis twice a cycle, all the filters were tested for the residual MC-LR concentration in filtered water at the end of stage 1 (6th Week) and stage 3 (14th Week). The experiment was performed for three different initial MC-LR concentrations viz. 5 µg/L, 20 µg/L and 50 µg/L. The significance of this study was to check the performance of the filter adsorbents with and without bioaugmentation for different seasons where MC-LR concentration varies. Fig. 7 (A) and (B) shows the residual MC-LR obtained for various initial concentration of MC-LR for physical and bioadsorption phase, respectively. Sand and Fe filter failed to remove >20% MC-LR, even at the lowest tested initial MC-LR concentration of 5 µg/L. Fig. 7 (C) shows the bar chart graph representing average MC-LR removal due to physical adsorption (black) and bio-adsorption (green). GO filter performed best among all the filter even at the highest initial MC-LR concentration of 50 µg/L, removing 77% and 82% MC-LR in stage 1 and stage 3, respectively.

On an average, the mean removal efficiency of 71.2 ± 8.1% and 86.0 ± 11.7% was observed for FeGO filter when GO was coated over Fe-coated sand for stage 1 and stage 3 filter operation (Table 2), respectively. From this, it can be inferred that the GO coating over Fe-coated sand has remarkably enhanced the MC-LR adsorption by >70% and >50% in stage 1 and stage 3 filter operation. This further strengthens the factor of 'pi-pi interaction' and 'C-O-C group interaction' with –COOH and NH_2 group of MC-LR molecule that can be held responsible for higher MC-LR adsorption or molecule transformation (discussed more in detail in next section). Overall, average enhancement of 14.8%, 32%, 38%, 3.5% and 47% in MC-LR removal due to bioaugmentation (stage 3) was observed for FeGO, Fe, Sand, GO and rGO, respectively. It shows that except GO, rest all adsorbents shown enhanced performance in MC-LR removal, possibly by biodegradation.

In general, it can be inferred that the carbon atom coated over sand material such as GO, not only enhanced the MC-LR removal but
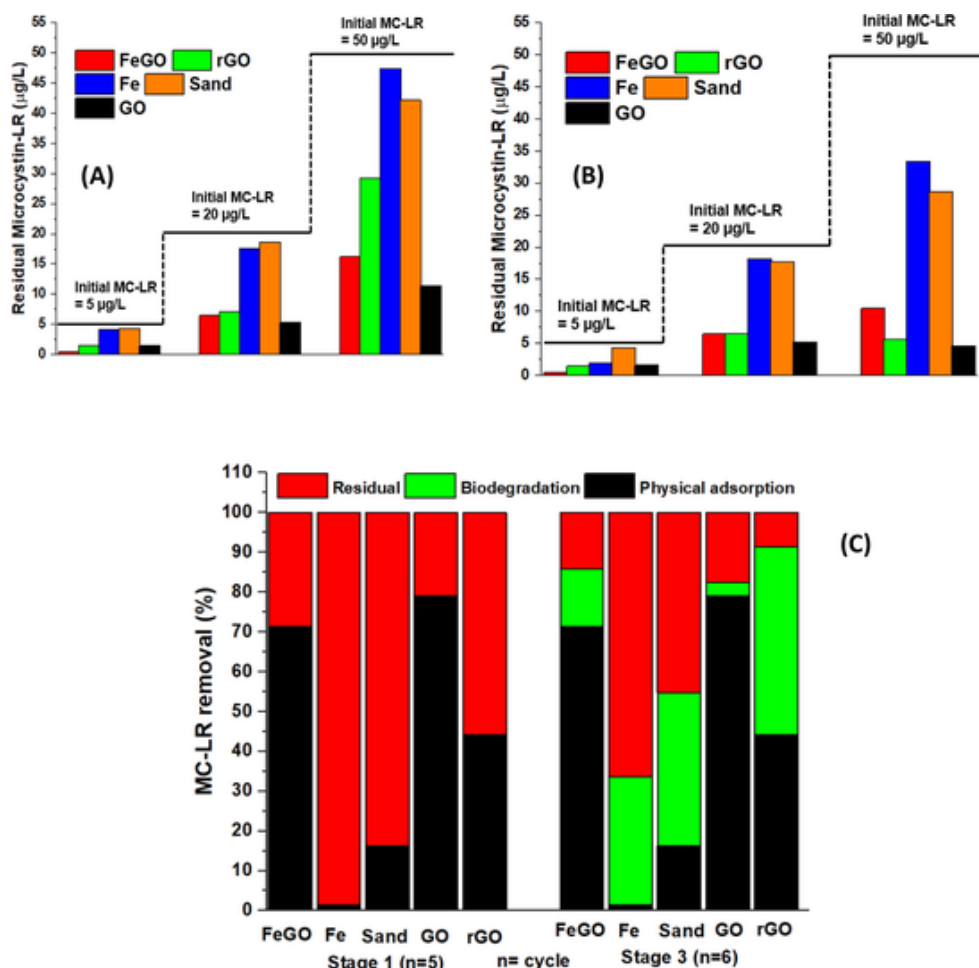
Fig. 7. Microcystin-LR removal by different synthesized filter media tested at three different concentration for A) stage 1 and B) Stage 3, and C) Microcystin-LR removal by different synthesized sand media for both stages of filter operation (Stage 1: 5 weeks/cycles and Stage 3: 6 weeks/cycles) (rGO: reduced graphene oxide, GO: Graphene oxide, FeGO: Iron coated on graphene oxide coated sand, Fe: Iron coated sand).

also maintained a good adsorption rate (>80% MC-LR removal at a residence time <25 min). This could also be related to the results of our previous study where graphitized sand (>65% carbon atoms based on atomic percentage value), synthesized using the brewery effluent sugar solution achieved a similar removal efficiency to GO [27]. A comparative study of various sand filters is presented in our previous published work (Kumar et al. 2020a). Though the removal efficiency achieved by carbon sub-micron particles coated sand (GO) for MC-LR and other water pollutants is higher (Table 3) than uncoated sand, yet the cost of synthesis can be an issue in future. However, a strong saturation adsorption capacity (discussed in a later section) and hence a higher breakthrough period can further improve the service life of sand material which can then be made techno-economically feasible. A preliminary techno-economic study was done based on the MC-LR adsorption capacity of GO-coated sand and sand adsorbent for the household purpose filter (according to Center for Affordable Water and Sanitation Technology or CAWST biofilter specification version 10.0). It was found that the GO-coated sand filter was economical (¾ th price to that of sand household filter (~2800 CAD[1]/annum)). The frequency change in the filter media as calculated for the sand filter was just 6 days as compared to over 70 days for the GO filter. A brief calculation table is presented in the supplementary section.

In the current study, only two MC-LR degraders: *Arthrobacter ramosus* and *Bacillus* sp. were chosen and co-cultured with the native bacterial species isolated from the filtration unit of DWTP and hence, any inferences on the possibility of more MC-LR removal (stage 3 filter operation assisted by biodegradation) that could have been achieved otherwise, is always subjective and most likely to be true. Nevertheless, the highest MC-LR improvement due to bioaugmentation was reported for the rGO filter (by 47%) which was also evident from the PCA analysis (Fig. 5 (B)) where rGO point variable moved closer to the MC-LR removal eigenvector in stage 3 filter operation. Since the GO and FeGO grains were tested for the biofilm formation (Section 3.4) and survivability test for GO particles (section 3.1) before coating them over sand, it could be interpreted that the MC-LR and other water quality parameters were responsible for the decrease in cell viability in the formed biofilm resulting in a low MC-LR removal performance. Another possibility could be the incompatibility issues of co-culture growth mode for MC-LR-degraders with native bacterial species that outcompeted the former. The toxicity and the degradation mechanism were not deciphered in the current study and hence it would be interesting to understand the by-product toxicity.

3.9. MC-LR interaction with the adsorbents: A chemistry point of view

Fig. 8 depicts a Venn diagram showing common chemical interaction factors for every adsorbent material that could be held responsible for the MC-LR adsorption. Table 4 shows the chemical interaction fac-
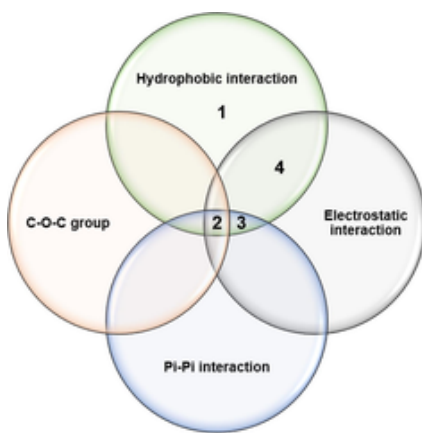
---

[1] CAD = Canadian Dollar

Adsorbent	Designated number	Combination
Sand		No
Fe	1	A
GO	2	A+B+C+D
rGO	3	A+C+D
FeGO	4	A+D

Fig. 8. Venn-diagram showing common chemical interaction factors for every adsorbent materials.

Table 4
Type of chemical interaction responsible for MC-LR adsorption.

Reference code	Type of interactions	Evidence
A	Hydrophobic interaction	Zeta potential
B	Epoxy/Ether group (C-O-C)	FT-IR
C	pi-pi interaction (Π-Π)	FT-IR and comparison of result for MC-LR removal between GO/rGO and Fe/Sand
D	Electrostatic interaction	Zeta analysis

tors and their evidence with the reference code to study Fig. 8. Fe-coated sand adsorbent performed extremely poor (<5% MC-LR removal in phase 1) as compared to other adsorbents. The only contributing factor that could be held responsible for the MC-LR adsorption is electrostatic interaction due to electropositive surface properties (MC-LR molecule is negatively charged at pH 7). The reason for an average performance of rGO-coated sand adsorbent in terms of MC-LR removal (<45% MC-LR removal) as compared to its oxidized form (GO-coated sand: 79% MC-LR removal) could be attributed to the lack of C-O-C group due to less oxygen atom in the chemical structure of the former (refer EDX results: Table 2). Since the MC-LR molecule in its native form shows two –COOH groups and one –NH$_2$ group, and the fact that the C-O-C group assists in the transformation of the above two chemical groups to other products, could be held responsible for the above difference in MC-LR removal.

The common factor for GO and rGO that can be held responsible for the removal of MC-LR include electrostatic interaction, pi-pi interaction and hydrophobic interaction. On the other hand, FeGO shows the most electropositive surface among all the synthesized adsorbent material and due to more hydrophobic (Supplementary Fig. S11), the combined factor showed strong factors in MC-LR removal as FeGO achieved >71% MC-LR removal during stage 1 filter operation. However, among all the four factors as depicted in Table 4, electrostatic interaction could be the weakest among all for the promotion of MC-LR adsorption as the sand surface was found to be less electropositive than Fe-coated sand and yet the latter showed 30% less MC-LR removal than the former. Equally, the factor of BET surface area cannot be ignored as the physical adsorption also depends on the surface area availability for the pollutant adsorption through Van der Waals' force (BET value of GO vs. Sand discussed earlier).

3.10. Regeneration and reusability study of the filter media

Fig. 9 shows the breakthrough curve obtained for all the filters using Rhodamine-B as an adsorbate. The highest breakthrough time was observed for GO filter (30 min) followed by rGO (23 min), FeGO (22 min), Fe (7 min) and sand (7.3 min). The highest saturation adsorption (Wsat) was determined for the GO filter (10.4 mg/kg) followed by rGO (7.4 mg/kg) which was 7.4 and 5.3 times more than the sand filter. After three cycles of regeneration, GO filter media still retained the Wsat of 8.7 mg/kg, declining by just 16% as compared to a maximum decrease of 54% for Fe followed by 38% for FeGO and 24% for rGO coated sand media. The above results suggest high reusability aspects of GO filters that can be sustained for a longer period (operational time) as compared to the sand media. Though a model dye 'Rhodamine-B' was used to obtain the adsorption parameters (adsorption constant and saturation capacity) for different filter media, still a more comprehensive study on the adsorption kinetics using 'MC-LR' should be done to better understand the adsorption strength of an adsorbent. This will help the DWTP operators to judge the kind of adsorbent to be used, especially when many adsorbents possess equal MC-LR removal potential, tested only a few times in the laboratory. Some other research gaps and current scenarios are discussed in the supplementary section.
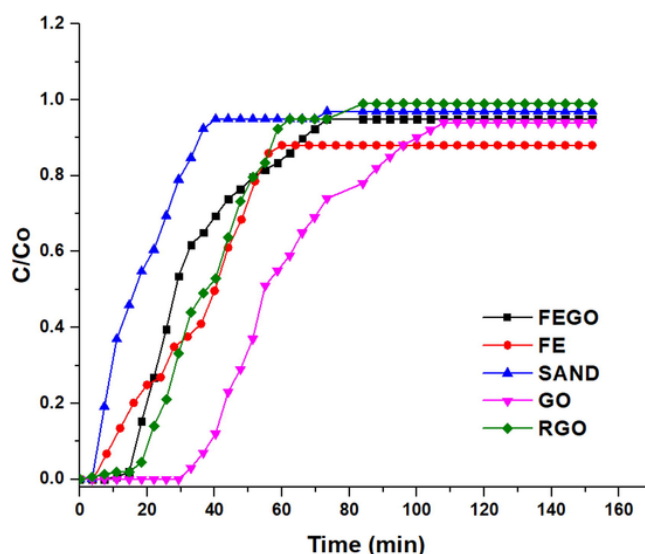

Fig. 9. Breakthrough time curve for all the synthesized filter media (rGO: reduced graphene oxide, GO: Graphene oxide, FeGO: Iron coated on graphene oxide coated sand, Fe: Iron coated sand).

4. Conclusion

Carbonization in form of graphene oxide (GO) and reduced graphene oxide (rGO) over sand grains improved the physical adsorption of Microcystin-LR (MC-LR) by 63% and 28%, respectively. Removal of other water quality parameters (WQPs) including metal ions, dissolved organic carbon and organic nitrogen components (NH_4-N, NO_2-N and NO_3-N) enhanced by coating GO and rGO over the sand media. The synthesized GO and rGO dose were optimized as 420 mg/L and 540 mg/L, respectively, before coating them over sand that maintained a survivability rate of at least 60% for the tested MC-LR-degraders: *Arthrobacter ramosus* and *Bacillus* sp. The most efficient filter according to the Principal Component Analysis (PCA Loading scores) was the GO-coated sand filter under physical adsorption phase and rGO-coated sand filter under the bioadsorption phase that was potent in removing most of the WQPs, including MC-LR by up to 91% (initial MC-LR: 50 µg/L). Regeneration of GO filter media showed around 7 times better saturation adsorption capacity (10.4 mg/kg) than the uncoated sand media. The more electropositive surface as compared to the uncoated sand surface was found to be effective in MC-LR adsorption with enhanced performance (except iron oxide coated sand media). The presence of chemical groups such as C-O-C, C=C (pi-pi interaction) on mesoporous graphene oxide planes were found responsible for active adsorption of MC-LR on GO and FeGO (Fe + GO) coated sand media. Bioaugmentation of MC-LR-degraders further elevated the performance of water pollutant removal where the MC-LR removal efficiency increased by 14.6%, 32%, 38%, 3.5% and 47% for filters: FeGO, Fe, sand, GO and rGO, respectively. Overall, the water treatment study using bio-optimized GO/rGO-coated sand media, carried by integrating various WQPs in real source water (lake water), has the potential to break frontiers for the biofiltration studies providing a modern approach to drinking water treatment facilities.

Declaration of Competing Interest

The authors declare that they have no known competing financial interests or personal relationships that could have appeared to influence the work reported in this paper.

Acknowledgments

Appendix A. Supplementary data

Supplementary data to this article can be found online at https://doi.org/10.1016/j.cej.2020.125398.

References

[1] M Elbana, F Ramírez de Cartagena, J Puig-Bargués, Effectiveness of sand media filters for removing turbidity and recovering dissolved oxygen from a reclaimed effluent used for micro-irrigation, Agric. Water Manag. 111 (2012) 27–33, doi:10.1016/j.agwat.2012.04.010.

[2] M Nageeb, Adsorption technique for the removal of organic pollutants from water and wastewater, Organic Pollutants – Monitoring, Risk and Treatment, 2013.

[3] P Kumar, K Hegde, S K Brar, M Cledon, A Kermanshahi-pour, A Roy-Lachapelle, R Galvez-Cloutier, Co-culturing of native bacteria from drinking water treatment plant with known degraders to accelerate microcystin-LR removal using biofilter, Chem. Eng. J. 383 (2020), doi:10.1016/j.cej.2019.123090.

[4] I Ali, A A Basheer, X Y Mbianda, A Burakov, E Galunin, I Burakova, V Grachev, Graphene based adsorbents for remediation of noxious pollutants from wastewater, Environ. Int. 127 (2019) 160–180, doi:10.1016/j.envint.2019.03.029.

[5] T J M Fraga, M N Carvalho, M G Ghislandi, M A Motta Sobrinho, d, Functionalized graphene-based materials as innovative adsorbents of organic pollutants: a concise overview, Braz. J. Chem. Eng. 36 (1) (2019) 1–31, doi:10.1590/0104-6632.20190361s20180283.

[6] N Yousefi, K K W Wong, Z Hosseinidoust, H O Sørensen, S Bruns, Y Zheng, N Tufenkji, Hierarchically porous, ultra-strong reduced graphene oxide-cellulose nanocrystal sponges for exceptional adsorption of water contaminants, Nanoscale 10 (15) (2018) 7171–7184, doi:10.1039/c7nr09037d.

[7] L Rizzo, A Fiorentino, M Grassi, D Attanasio, M Guida, Advanced treatment of urban wastewater by sand filtration and graphene adsorption for wastewater reuse: Effect on a mixture of pharmaceuticals and toxicity, J. Environ. Chem. Eng. 3 (1) (2015) 122–128, doi:10.1016/j.jece.2014.11.011.

[8] Z Ding, X Hu, V L Morales, B Gao, Filtration and transport of heavy metals in graphene oxide enabled sand columns, Chem. Eng. J. 257 (2014) 248–252, doi:10.1016/j.cej.2014.07.034.

[9] L Hou, Q Feng, Y Wang, X Yang, J Ren, Y Shi, Z Zhang, Multifunctional hyaluronic acid modified graphene oxide loaded with mitoxantrone for overcoming drug resistance in cancer, Nanotechnology 27 (1) (2015), doi:10.1088/0957-4484/27/1/015701 015701.

[10] D G Bourne, R L Blakeley, P Riddles, G J Jones, Biodegradation of the cyanobacterial toxin microcystin LR in natural water and biologically active slow sand filters, Water Res. 40 (6) (2006) 1294–1302, doi:10.1016/j.watres.2006.01.022.

[11] L Ho, T Meyn, A Keegan, D Hoefel, J Brookes, C P Saint, G Newcombe, Bacterial degradation of microcystin toxins within a biologically active sand filter, Water Res. 40 (4) (2006) 768–774, doi:10.1016/j.watres.2005.12.009.

[12] V S Stenkamp, M M Benjamin, Effect of iron oxide coating on sand filtration, J. Am. Water Works Assoc. 86 (8) (1994) 37–50, doi:10.1002/j.1551-8833.1994.tb06236.x.

[13] B Ø Hansen, P Kwan, M M Benjamin, C-W Li, G V Korshin, Use of iron oxide-coated sand to remove strontium from simulated hanford tank wastes, Environ. Sci. Technol. 35 (24) (2001) 4905–4909, doi:10.1021/es0108990.

[14] P Kumar, K Hegde, S K Brar, M Cledon, A Kermanshahi-pour, A Roy-Lachapelle, R Galvez-Cloutier, Biodegradation of microcystin-LR using acclimatized bacteria isolated from different units of the drinking water treatment plant, Environ. Pollut. 242 (2018) 407–416, doi:10.1016/j.envpol.2018.07.008.

[15] J Mehlig, Colorimetric Determination of Copper with Ammonia, Ind. Eng. Chem. Anal. Ed. 13 (8) (1941) 533–535, doi:10.1021/i560096a006.

[16] W B Fortune, M G Mellon, Determination of Iron with o-Phenanthroline: A Spectrophotometric Study, Ind. Eng. Chem. Anal. Ed. 10 (2) (1938) 60–64, doi:10.1021/ac50118a004.

[17] APHA, AWWA, WPCF. 1998. Standard methods for the examination of water and wastewater,19th Ed., Washington, D.C.

[18] A Roy-Lachapelle, S V Duy, G Munoz, Q T Dinh, E Bahl, D F Simon, S Sauvé, Analysis of multiclass cyanotoxins (microcystins, anabaenopeptins, cylindrospermopsin and anatoxins) in lake waters using on-line SPE liquid chromatography high-resolution Orbitrap mass spectrometry, Anal. Methods 11 (41) (2019) 5289–5300.

[19] W Hu, C Peng, W Luo, M Lv, X Li, D Li, C Fan, Graphene-based antibacterial paper, ACS Nano 4 (7) (2010) 4317–4323, doi:10.1021/nn101097v.

[20] Y L Li, A Deletic, L Alcazar, K Bratieres, T D Fletcher, D T McCarthy, Removal of Clostridium perfringens, Escherichia coli and F-RNA coliphages by stormwater biofilters, Ecol. Eng. 49 (2012) 137–145, doi:10.1016/j.ecoleng.2012.08.007.

[21] V Singh, D Joung, L Zhai, S Das, S I Khondaker, S Seal, Graphene based materials: Past, present and future, Prog. Mater Sci. 56 (8) (2011) 1178–1271, doi:10.1016/j.pmatsci.2011.03.003.

[22] M M Benjamin, R S Sletten, R P Bailey, T Bennett, Sorption and filtration of metals using iron-oxide-coated sand, Water Res. 30 (11) (1996) 2609–2620, doi:10.1016/s0043-1354(96)00161-3.

[23] W Gao, M Majumder, L B Alemany, T N Narayanan, M A Ibarra, B K Pradhan, P M Ajayan, Engineered graphite oxide materials for application in water purification, ACS Appl. Mater. Interfaces 3 (6) (2011) 1821–1826, doi:10.1021/am200300u.

[24] A Doepke, C Han, T Back, W Cho, D D Dionysiou, V Shanov, W R Heineman, Analysis of the electrochemical oxidation of multiwalled carbon nanotube tower electrodes in sodium hydroxide, Electroanalysis 24 (7) (2012) 1501–1508, doi:10.1002/elan.201200105.

[25] M Teixidó, J J Pignatello, J L Beltrán, M Granados, J Peccia, Speciation of the Ionizable Antibiotic Sulfamethazine on Black Carbon (Biochar), Environ. Sci. Technol. 45 (23) (2011) 10020–10027, doi:10.1021/es202487h.

[26] Y Wang, Z Li, C Tang, H Ren, Q Zhang, M Xue, J Jiang, Few-layered mesoporous graphene for high-performance toluene adsorption and regeneration, Environ. Sci. Nano 6 (10) (2019) 3113–3122, doi:10.1039/c9en00608g.

[27] P Kumar, H Rehab, K Hegde, S K Brar, M Cledon, A Kermanshahi-pour, R Y Surampalli, Physical and biological removal of microcystin-LR and other water contaminants in a biofilter using manganese dioxide coated sand and graphene sand composites, Sci. Total Environ. 703 (2020), doi:10.1016/j.scitotenv.2019.135052.